Future Energy
Open Access Journal
ISSN 2832-0328

November 2023| Volume 02 | Issue 04 | Pages 01-09

Journal homepage: https://fupubco.com/fuen

https://doi.org/10.55670/fpll.fuen.2.4.1

Future Publishing LLC

Article

Seasonal variation of surface energy balance over Mubi northeastern Nigeria during 2000-2020

Abubakar Saidu Umar[1]*, Adam Usman[2]

[1]Department of Pure and Applied Physics, Adamawa State University, Mubi, Nigeria
[2]Department of Physics, Faculty of Physical Science, Modibbo Adama University, Yola, Nigeria

ARTICLE INFO

Article history:
Received 01 January 2023
Received in revised form
29 January 2023
Accepted 01 February 2023

Keywords:
Energy, Temperature, Heat, Surface, Mubi

*Corresponding author
Email address:
abuumarsaidu@gmail.com

DOI: 10.55670/fpll.fuen.2.4.1

ABSTRACT

Several studies have been undertaken on surface energy balance (SEB) at various places in the world, but none have been undertaken for Mubi, Northeastern Nigeria. In the effort of consideration, this study aims to evaluate the seasonal variation of SEB in Mubi, with emphasis on the observational data from 2000 to 2020. Evaluation of seasonal variations was executed using time series analysis to find out the impact of precipitation, evapotranspiration, soil, and air temperature changes on SEB components. It was found that the SEB components variations of sensible heat (H) had a maximum value of 1035.13 Wm^{-2} in the dry season, in the month of December, while a minimum value of -104.13 Wm^{-2} during the rainy season, in the month of July; latent heat (LH), had a peak value of 5243.46 Wm^{-2} in the dry season in the month of April, while in the rainy season, the lower value was found to be 2460.6 Wm^{-2}, in the month of August; soil heat (G) had minimum and maximum values of 886.43 Wm^{-2} in March and 275.25 Wm^{-2} in August respectively; and net radiative (R_n) varies roughly between the highest month in March with 2809.35 Wm^{-2} (rainy season months) and lowest month in August with 6879.69 Wm^{-2} (dry season months). It was also found that precipitation, evapotranspiration, soil, and air temperature follow the same trend with some SEB results, affirming their dependency on each other. Therefore, it is expected that this study will help to understand the amount of energy received or emitted in the Mubi region. Along with the main work, some recommendations were made by researchers on some applications of SEB to the community.

1. Introduction

It is highly essential to understand the interaction between the Earth and the atmosphere, which mainly links to the principle of energy conservation, called surface energy balance. SEB has been widely used to evaluate and compare the strength of the various factors affecting Earth's Surface. SEB principle conditions that the amount of energy arriving at the Earth's surface must equal the energy leaving the Earth's surface over a period of time. Otherwise, the energy is imbalanced. Solar radiation is the only significant energy source on the Earth that is transformed into various energy fluxes after entering into the atmosphere and Earth's surface [1]. Most of these energies come in the form of heat absorbed by the Earth's surface. In such processes, the resulting energy goes toward heating the Earth's surface by warming up sub-surfaces, Earth's atmosphere, and water bodies, which are later emitted back to the atmosphere. SEB establishes the state of the Earth's environment and responds to changes in the various energy transformation processes to account for all energy at the surface. Surface energy balance models are based on balancing net radiation with ground heat flux, sensible heat flux, and latent heat flux assuming that heat advection is negligible [2, 3] expressed as:

$$R_n = G + H + LH \quad (1)$$

where R_n is the net radiation flux (Wm^{-2}), G is the soil heat flux (Wm^{-2}), H is the sensible heat flux (Wm^{-2}), and LH is the latent heat flux (Wm^{-2}). The equation states that the net radiation flux received at the Earth's surface must either warm or cool the air above the Earth's surface (sensible heat flux), evaporate water bodies (latent heat flux), or warm or cool the soil (soil heat flux). As previously mentioned in equation (1), incoming net radiative flux (R_n) equals the combination of sensible heat (H), latent heat (LH), and soil heat (G) fluxes; the following are details explanations of individual's flux.

1.1 Net radiation flux (R_n)

The net radiation is the amount of heat energy delivered to do work at the surface of the earth. Solar radiation (short

and longwave radiation) are input energies to the surface energy balance. These energies, directly or indirectly, are the results of nuclear interactions occurring on the solar surface and is equal to the total available energy for the occurrence of the Earth's surface and atmospheric processes [4, 5]. Basically, solar radiation has two acting parts: one is incoming (downward Rs↓) radiation on Earth's surface that depends on the atmospheric transitivity, solar constant, solar altitude, and incidence angle, and another part are outgoing (upward Rs↑) that is reflected back to space due to the combined effect of surface, clouds, aerosol, gases, etc [1]. Therefore, surface net radiation (Rn) in the one-source surface energy balance model is estimated from the sum of the difference between the incoming and the reflected outgoing shortwave solar radiations (0.15–5 μm) and the difference between the downwelling atmospheric and the surface emitted and reflected longwave radiations (3–100 μm) [6]:

$$R_n = (1-\alpha)R_{global} + \varepsilon_s\varepsilon_a\sigma {T_a}^4 - \varepsilon_s\sigma {T_s}^4 \quad (2)$$

where α is the surface albedo. Surface albedo is a critical parameter that controls surface energy balance [7]. Albedo is the fraction of incoming radiation attenuated by reflection processes in the atmosphere, with values ranging from 0 to 1 for the lowest and highest reflection, respectively. Most of the estimated global solar radiations are often corrected by albedo, which contributes greatly to estimating the global average amount of incoming solar radiation onto a particular place on the Earth's surface. This can affect surface albedo and radiation fluxes, leading to a local temperature change and, eventually, a vegetation response [8]. This implies that the global solar radiation received on the Earth's surface was more than the reflected radiation lost into space [9]. Although the global annual mean land albedo varies from 0.18–0.26 [10,11], climate, biogeochemical, hydrological, and weather forecast models require regional surface albedo with an absolute accuracy of 0.02–0.05 for snow-free and snow-covered land [11]. For this study, a typical constant value of 0.03 is taken based on Bastiaanssen [12], the value also corresponds to a value obtained by [7]. R_{global} is the global solar radiation in W m^{-2}, εs is the surface emissivity, εa is the atmospheric emissivity estimated as a function of vapor pressure, and σ is the Stefan–Boltzmann constant. Surface emissivity is computed using an empirical equation by Tasumi [13], based on soil and vegetative thermal spectral emissivities housed in the MODIS UCSB Emissivity Library [14].

$$\varepsilon_a = 0.95 + 0.01\,\mathrm{LAI} \quad \text{for LAI } 3 \leq 1 \quad (3)$$

ε_a=0.98 when LAI>3, where LAI (m^2 m^{-2}) leaf area index; the ratio of the total leaf area for the surface one side of leaves per unit of ground area. LAI is an indicator of biomass and canopy resistance to vapor flux and is computed using an empirical equation stemming from Bastiaanssen [14, 15].

$$\mathrm{LAI} = -\ln[(0.69 - \mathrm{SAVIID}/0.59)/0.91 \quad (4)$$

where, for Landsat images, SAVI 6 is based on the top of atmosphere reflectance of bands 3 and 4. Several different methods have been proposed to estimate atmospheric emissivity, but according to Brutsaert [16], atmospheric emissivity is given as:

$$\varepsilon_a = 9.2 \times 10^{-6} {T_a}^2 \quad (4)$$

1.2 Soil heat flux (G)

Soil heat flux (G) is the amount of heat transfer in vegetation and soil through molecular conduction. It is determined by the soil thermal conductivity and heat capacity which both depend on properties such as soil texture, i.e. fractions of sand, loam, and clay particles, and soil water content [17]. It also affects soil physical processes such as soil evaporation and aeration, chemical reactions in the soil, and biological processes such as seed germination, seedling emergence and growth, root development, and microbial activity [18]. Soil heat flux (G), which is determined by the thermal conductivity of the soil and the temperature gradient of the topsoil, can be derived using the method developed by Kustas and Daughtry [19] and Bastiaanssen [15], which is a function of surface albedo, surface temperature, and normalized difference vegetation index (NDVI) written as [20]:

$$G = R_n T_s(0.0038 + 0.0074\alpha)(1 - 0.98(NDVI)^4) \quad (5)$$

where the normalized difference vegetation index, NDVI.
Vegetation cover is one of the most important biophysical factors in determining SEB through NDVI. NDVI is defined as a ratio of the difference in reflectivity of the near-infrared and red bands to their sum:

$$NDVI = \frac{rNIR - rRED}{rNIR + rRED} \quad (6)$$

NDVI is a widely used technique to detect land use land cover change, especially changes in vegetation area and its pattern [21]. NDVI values range from 1 to -1. Sparse vegetation (e.g. shrubs, meadows, and pastures) are expressed by values of 0.2 – 0.5 [22]. Also, 0.2< NDVI<0.5, assumed to be a mix of bare soil and vegetation [23], 0.2-0.3 NDVI value represents shrub and grassland, 0.3-0.4 indicates sparse and unhealthy forest whereas >0.4 NDVI value represents healthy and dense vegetation [21]. High values (from 0.6 to 0.9) correspond to areas with dense vegetation, such as forest or agricultural vegetation, in the productive phase [24]. In this paper, the best features for the Mubi region were described to vary from 0.1 to 0.5 due to the fractional land cover vegetation prevailing almost 80% cropland. The NDVI classification is indicated in Table 1.

Table 1. The NDVI classification [25]

Class/Feature	NDVI Range
Water	-1 ≤ - 0.014
Build-up	0.015 - 0.09
Barren land	0.10-0.20
Shrub and grassland	0.21-0.30
Sparse vegetation	0.31-0.40
Dense vegetation	0.41 - ≤ 1

1.3 Sensible heat flux (H)

The sensible heat flux is the exchange of energy between the surface and the atmosphere obtained from the

temperature difference between the surface and the atmosphere. Calculation of the sensible heat flux of the surface is done using an aerodynamic function:

$$H = \rho_{air} C_p \frac{dT}{r_{ah}} \quad (7)$$

Where, ρ_{air} is the air density in kg/m^3, C_p is the specific heat of air at constant pressure, which is equal to 1000 (J/kgK), dT is the indicator of temperature difference in Kelvin between two elevations near surfaces of z_1 and z_2, and r_{ah} is the aerodynamic resistance (m/s) available for the heat transfer between z_1 and z_2, which are considered 0.1 and 2 meters [4, 26, 27]. Aerodynamic resistance is affected by the surface roughness and is determined by vegetation height and structure, wind speed, and atmospheric stability [6]. Here, aerodynamic resistance is taken to be 2 s/m due to the roughness of the study area. Based on equation (7), the higher the temperature difference and the aerodynamic resistance, the larger the sensible heat flux. Also, Sensible heat flux is zero if the temperature difference or aerodynamic resistance is zero.

1.4 Latent heat flux (LH)

Latent heat flux is the flux of energy associated with the evaporation or transpiration of water from the Earth's surface to the atmosphere and vice versa [28], sometimes called evapotranspiration (ET). The primary controls on ET are energy inputs such as incoming solar radiation and the capacity of the air to hold more water vapor both from local water vapor (humidity) and from mixing with drier air controlled by wind speed [2]. This process cools the Earth's surface and moistens the atmosphere near the surface, which is why the estimation of ET is crucial for developing climatic, hydrological, bio-geophysical, and ecological models to predict the weather and climate or climate change [1]. The latent heat flux (LH) can be expressed as:

$$LH = R_n - G - H \quad (8)$$

The above said components of Earth's SEB are responsible for the heating or cooling of the land/soil (solar and thermal radiation), the heating and cooling of the air (sensible heat flux), and the evaporation of water from soil and vegetation (latent heat flux) [1]. From equation (1), when the amount of energy coming to the surface (R_n) equals the amount of energy leaving Earth's surface (G + H + LH), the surface is said to be in energy balance (zero), and the temperature remains constant. Also, if the sum of the energies in equation (1) is not equal to zero, then the resulting energy and temperature are said to be an imbalance. Moreover, if the incoming is more than the outgoing energy to the surface, then the energy is said to be positive imbalance and negative if the outgoing is more than the incoming energy. It is a negative imbalance because it contributes to global warming, while positive contributes to global cooling. Such processes have an essential role in regional weather, climate, and hydrosphere cycles, as well as in regulating urban heat redistribution [20]. Also, the exchange processes occurring at the land surface are of paramount importance for the re-distribution of moisture and heat in soil and atmosphere [29]. For the past decade, SEB has become a standard tool to study the exchange of energy between the Earth's surface and atmosphere. The research of SEB is often carried out in different places such as Jakarta and Neighboring regions by Ilhamsyah [30], metropolitan cities of India during the 2000–2018 winter seasons by Sultana and Satyanarayana [28], Greenland ice sheet by Liu [31], Naqu region of Qinghai-Tibet Plateau during 2005-2016 by Wang and Ma [32], lake Huron by Petchprayoon [33], tilled and non-tilled bare soils by Akuoko [34], tropical river Basin by Kumar et al. [35], semiarid environments by Small and Kurc [36], Storglacia¨ren, Sweden by Hock and Holmgren [37], urban park and its surroundings by Bäckström [38], two Sahelian surfaces by Verhoef et al. [39]. These studies motivated us to carry out such research in Mubi, Northeastern Nigeria, to benefit from the resources that SEB is disclosing. The application of energy balance to a wide mixture of agricultural crops and other vegetation is complex enough that there are still some areas of considerable empiricism and, therefore, the potential for local refinement [14]. At the same time, all physical, chemical, and biological processes respond to changes in conditions produced by changes in the SEB. In recent times of agricultural and settlement expansion, increase in human population, over-exploitation of natural resources, and intense flux of Earth's surface energy cause a serious threat to human beings, agriculture, and settlement. This is specifically true in Mubi. Hence, adequate information about SEB status is relatively scarce in Nigeria, particularly Mubi. Understanding and utilizing metamorphic trends, water vapor loss, precipitation, plant growth, drought monitoring, revegetating a barren area, irrigation scheduling, drainage practices, erosion, desertification, and global climate changes, among others, depends on SEB, and has yet to be fully exploited in Mubi. In an effort to fill this gap, this study aims to evaluate the seasonal variation of SEB in Mubi, with emphasis on the observational data from 2000 to 2020. Along with the main work, some recommendations were made by researchers on some applications of SEB to the community.

2. Method and materials

2.1 Study area

Mubi, Northeastern Nigeria, is within the foothills zone of Mandara Mountains terrains (characterized by hill landforms and flat plain land), at Longitude 13.125 and Latitude of 10.333 with an average altitude of about 650 m above sea level. Due to its topography and climate, which is dominated by crops, Mubi serves as one of the major agricultural regions in Nigeria and is one of the most important economic activities in the region, with about 65% of the total working population being engaged directly. The seasonal variations of Mubi were dry (in the months of November, December, January, February, March, and April) and rainy (in the months of May, June, July, August, September, and October) season. The estimated average temperature and precipitation in Mubi are respectively 28.83°C and 1,154.75 mm over the last 20 years. The highest and lowest temperatures, respectively, occur in April and August, while precipitation almost occurs in the rainy season.

2.2 Types and sources of data

Several parameters were acquired for this study. Some of them are literature based, while others were obtained from Meteoblue, as shown in Table 2. Mean daily global solar radiation, soil temperature (at 0-10cm depths), and air

temperature (at 10m height) historical weather simulation data used in this research, with a spatial resolution between 4 and 30 km for the Mubi location, were obtained from Meteoblue product for the period of 20 years (2000-2020). Although soil temperature may increase, decrease, or vary monotonically with depth, depending on the season and the time of the day [40, 41]**.** For this study, daily soil temperature data taken at the soil surface (0-10 cm) was adopted from the available data. These parameters are assumed to be homogeneous throughout the Mubi station and offer an opportunity to evaluate SEB and help understand the variability over time.

Table 2. Data used for the analysis

Type of parameters	Values	Source of data
Global solar radiation (R_{global})	Varies over time (Wm^{-2})	Meteoblue
Soil temperature (T_s)	Varies over time (°C)	Meteoblue
Air temperature (T_a)	Varies over time (°C)	Meteoblue
Albedo (α)	0.03	Dintwe, [7]
Soil emissivity (ε_s)	0.85	Estimated by study
Air emissivity (ε_a)	Varies over time (unit less)	Evaluated
Air density (ρ_{air})	1.225 kg m^{-3}	Constant
Specific heat capacity of air (C_p)	1000 J/kgK	Constant
Aerodynamic resistance (r_{ah})	2 s/m	Tang et al. [6]
NDVI	0.3	Bid [21]
Stefan–Boltzmann constant (σ)	$5.67 \times 10^{-8} W\ m^{-2}K^4$	Constant
Evapotranspiration	Varies over time (mm)	Meteoblue
Precipitation	Varies over time (mm)	Meteoblue

2.3 Method of data analysis and presentation

As shown in Table 2, the data acquired from literature and Meteoblue weather station for Mubi are all known constants, dependents, and independent variables that are accordingly derived, evaluated, or directly computed into equations 1 to 8 of SEB fluxes. The data obtained went through pre-processes by averaging daily data to monthly and annual time intervals before calculations were taken. These methods of calculating SEB components are purely empirical and were carried out basically to establish time series to capture the trends associated with changes. To present the result obtained from calculations, we selected dry and rainy seasons for typical weather conditions to analyze the variation of each component under SEB for the analysis, and to test whether the variability is in line with the evaluation. Application of time series analysis for annual and seasonal evidence of 2000 to 2020 periodicity was carryout using Mathematica software for the presentation of results.

3. Result and discussions

It is very important to note that the monthly potential combination of net radiative heat (R_n), sensible heat (H), latent heat (LH), and ground heat (G) fluxes equated monthly SEB. Therefore, the results of each of these parameters are discussed for better understanding.

3.1 Variations of air and soil temperatures on the SEB

Soil temperature is a measure of soil internal energy or heat content and changes in the heat gained or lost by the soil [42]. Soil temperature is one of the most important factors that affect soil heat storage, soil heat flux, soil water flux, seed emergence, nutrient transformation, transport, uptake, and plant growth [43] plays a major role in ensuring crop productivity, sustainability and control of biological and biochemical processes which invariably affects soil organic matter formation, fertilizer efficiency, seed germination, plant development, the ability of the plant to survive during the dry season, nutrient uptake and decomposition, and disease and insect occurrence [44-48]. Furthermore, increased soil temperatures will have a direct impact on water demand and crop yield [49], shift spring temperature threshold, indicating potentially longer vegetative period and earlier yield and subsequent secondary crop yield [50], and major changes in the morphology of the plant was evident [51]. Plants stop growing when the soil temperature becomes too cool, and some stop growing when the soil temperature is too hot. The optimum range of soil temperature for plant growth is between 20 and 30°C, and the rate of plant growth declines drastically when the temperature is less than 20°C (sub-optimal) and above 35°C (supra-optimal) [48]. Based on this, it is observed that the soil temperature values of Mubi were considerably stable, as expected for crops (Figure 1). Being able to determine temperature differences in Mubi is important in the discussion of SEB.

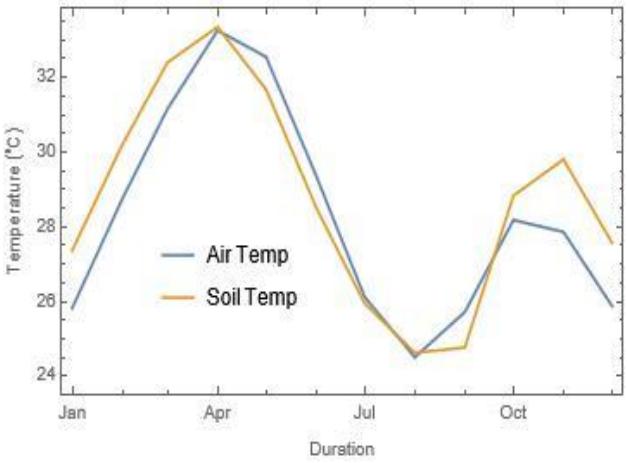

Figure 1. Time series of monthly variations of air and soil temperature for Mubi during 2000-2020

As shown (Figure 1), the air and soil temperature trend is almost the same, but the difference has obvious seasonal

changes. Both air and soil temperature in November has a higher trend, which gradually decreases before reaching a peak in April. The soil temperature from October to April is higher than the air temperature (dry season), and the air temperature is higher than the soil temperature from May to September (rainy season). The trend values of temperature difference during dry and rainy seasons period of the year revealed interesting spatial variability patterns. As a result, groundwater loss is greater as drier and warmer conditions in Mubi increase evaporative losses in the rainy season. The losses were less prominent in the dry season (that is from October to April than in the months in the dry season. The differences indicate why temperature highlights the importance of SEB. In both cases, the month of April had the highest temperatures (33.34 °C), whereas the lowest was in the month of August (24.63°C). Results also demonstrated that during the dry (November to May), both soil and air temperatures were warmer than the rainy (May to October) seasons temperatures. The air temperature showed an opposite trend, with soil temperature being warmer than the air temperature in the dry season. Monthly, from January to April, the temperature increases higher and decreases from April to August, which then increases to the month of November, then decreases to January. January to December of each year indicates the temperature path reversal, creating seasonal and annual variations. In this situation, dry-season soils had a significantly higher temperature than rainy-season soils temperature. Accordingly, continual air and soil temperature variations depend on response to changes in Earth and atmospheric conditions of solar radiation, an increase of soil moisture content, air temperature, wind speed, rainfall, and others weather conditions. This phenomenon was due to the effects of weather conditions, which allow solar radiation to warm the Earth's surface. Therefore, the lower temperature of the surface of the Earth generally gains cold at a higher rate of rainfall than the Earth's surface in the dry season.

3.2 Variations of precipitation and evapotranspiration on the SEB

As shown in Figure 2, Mubi experiences average precipitation and evapotranspiration of 1,154.75 and 479.33 mm annually. The highest and the lowest monthly precipitation value of 276.31 mm is found in the month of August and 0 mm in the months of December, January, and February, respectively. At the same time, the highest and the lowest monthly evapotranspiration value of 85.89 mm are found in the month of September and 9.63 mm in the month of January, respectively. During the dry season, both precipitation and evapotranspiration in Mubi experience fewer magnitude variations than the associated rainy season values. A similar trend of precipitation and evapotranspiration variations was observed during this period of 20 years (Figure 2). These similarities are attributable to the changes in various climatic variables such as air and soil temperature, heat from solar radiation, rainfall infiltrated into the soil, crop residue covering the soil surface, snow cover, freezing, and thawing. Another reason could be the presence of a cloud, which may allow only a small part of solar radiation to reach the ground surface due to its ability to reflect a good part of the solar radiation [40, 41]. In the rainy season, this is not because of the input precipitation but due to the influence of the harmattan wind, which significantly reduces the amount of potential evapotranspiration [52].

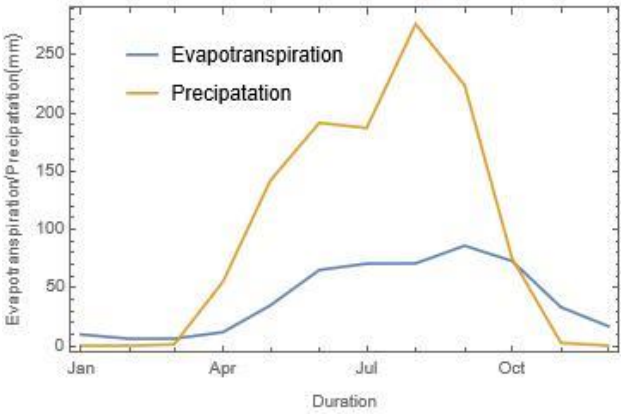

Figure 2. Time series of monthly variations of precipitation and evapotranspiration for Mubi during 2000-2020

The evapotranspiration (ET) increases with precipitation and contributes to the highest water loss or gain in SEB. The differences between them are wide in the rainy season, where ET is relatively small and thus contributes to a larger fraction in lowering R_n and LH (Figure 3). Higher values of ET occurred during the corresponding months of higher precipitation in Mubi. Here, ET is a collective term that includes evaporation from vegetation or any other moisture-containing living surface (transpiration) and evaporation from the water bodies and soil and is used to describe the loss of water from the Earth's surface to the atmosphere by the combined processes of evaporation and transpiration [53]. A thorough understanding of the factors controlling the energy balance of cropped soil enables making accurate estimates or predictions of evapotranspiration and irrigation water requirements [54]. While contributing to the surface energy balance, ET quantifies the water requirement for efficient water management [55-57], especially in sub-humid and humid climates [54]. According to the energy budget concept, when the surface is wet or heavily vegetated, net energy is mainly consumed by the evaporation and evapotranspiration of water in soil and vegetation [20]. In essence, if there is adequate water in the soil, the incoming solar radiation will be used for convective activities [52]. Moreover, an increase in soil moisture gives rise to increased evaporation from the soil surface, and a substantial part of net radiation goes into evaporation, which also gives rise to the observed low temperature [41], and increasing evapotranspiration can decrease the surface temperature of tree canopy [57, 58]. Atmospheric temperature is projected to increase with climate change, and it provides more energy to cause more evaporation [57]. Salman et al. [59] used simple water-balance equations and identified that when the temperature increases, it contributes to an increment in evapotranspiration, which leads to a large increase in crop water demand and a decrease in climatic water availability. With this, it is affirmed that evapotranspiration and precipitation are both important for balancing the effects of SEB in Mubi. Here, seasonal variation of precipitation and evapotranspiration often represents the amount of water

consumed from agriculture. Thereby significantly helping farmers in Mubi by projecting water management in farms.

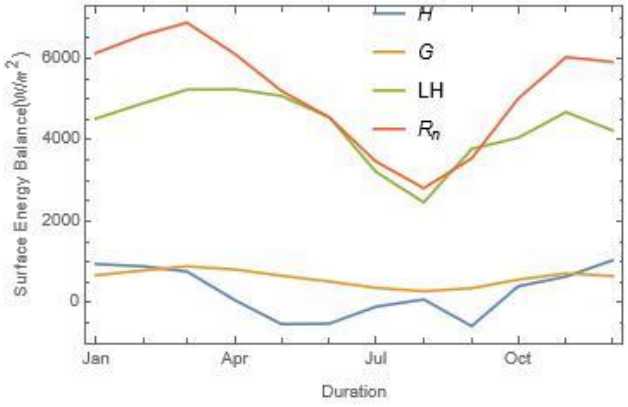

Figure: 3. Time series of monthly variations of sensible heat (H), latent heat (LH), soil heat (G), and net radiative fluxes during 2000-2020

3.3 Surface Energy Balance

Results for each SEB component of equations (2 to 8) are explained in this section. It is noted that each component of net radiative heat (R_n), sensible heat (H), latent heat (LH), and ground heat (G) fluxes are discussed separately as follows:

3.3.1 Net Radiative Flux

Net Radiation flux (R_n) is the component of SEB defined by equation 2. As shown in Figure 3, R_n over the entire 20 years appeared to be a very wide trend, varying roughly between the highest month in March with 2809.35 Wm^{-2} (rainy season months) and the lowest month in August with 6879.69 Wm^{-2} (dry season months). Here, R_n controlled most of the variations in SEB due to the large values of incoming global solar radiation energy onto the Earth's surface. As the short wave radiation balance is lower due to high albedo (equation. 1), air and soil temperatures tend to be low. Its trend follows the same pattern with temperature variations (Figure 1). Implying that higher R_n defines higher temperature at the same time. Principally, the differences of R_n play major role in SEB than others components. Explaining that R_n is higher than any other energy in SEB. As shown, both the R_n and LH in dry and rainy seasons have the same diurnal variation trend as that of air and soil temperatures (Figure1). This revealed to us that they depend on each other. Meanwhile, during the dry season, a large amount of R_n reaches the Earth's surface from the atmosphere leading to the temperature differences between the Earth and the atmosphere. Therefore, the high amount of R_n found in the Mubi region during the dry season and low in the rainy season may have a great impact on balancing energy between the Earth's surface and atmosphere.

3.3.2 Soil heat flux (G)

As shown in Figure 3, the minimum and maximum values G are respectively 886.43 Wm^{-2} in the months of March and 275.25 Wm^{-2} in August. At the same time, R_n, LH, and G follow the same trend but at different values. The reason for this phenomenon is that solar radiation inhibits heat exchange between the atmosphere and the underlying Earth's surface, which strongly impacts evapotranspiration and precipitation (Figure 2). Comparatively, the contribution of the G to SEB is lower than that of R_n and LH throughout these 20 years.

3.3.3 Sensible heat flux (H)

As shown in Figure 3, during the dry season, in the month of December, H had maximum value of 1035.13 Wm^{-2}, while the minimum value during the rainy season, in the month of July is -104.13 Wm^{-2}. H values are the highest positive values during the months of October, November, December, January, February, March, April, and August mostly occur in the rainy season. While negative values were observed in the rainy season in the months of May, June, July, and September. It is positive because the incoming energy is absorbed by the soil and negative when emitted to the atmosphere. Sensible heat flux is caused by an interaction between the Earth's surface and the atmosphere, whose values are mainly determined in terms of thermal differences and wind speed.

3.3.4 Latent heat flux (LH)

As shown in Figure 3, in the dry season, the peak value of LH is 5243.46 Wm^{-2}, observed in the month of April, while in the rainy season, a lower value was found to be 2460.6 Wm^{-2}, in the month of August. The LH is usually characterized by the soil water contents on the Earth's surface. As shown (Figure 3), LH is in the opposite trend with precipitation and evapotranspiration (Figure 2). Therefore, the lower the value of LH, the higher the water contents on Earth's surface (precipitation). LH has a great impact on determining and detecting seasonal variation in Mubi.

3.4 Surfaces energy imbalance

Surface energy imbalance is the method of evaluating whether the energy that is coming onto the Earth's surface is the same as that is going out to the atmosphere. It is obtained by subtracting all outgoing energy fluxes from all incoming energy fluxes. That is R_n - LH+G+H. Surface energy imbalance requires that the G+H+LH be equivalent to R_n. When both sides are the same (subtracted to be zero), the interaction between the Earth's surface and the atmosphere is balanced, called SEB. As shown in Figure 4, the energy exchange between the atmosphere and the Earth's surface is minimal. The result shows close agreement with SEB of +/- 2×10^{-12} to 4×10^{-12}. Therefore, the result is in agreement with SEB (equation 1).

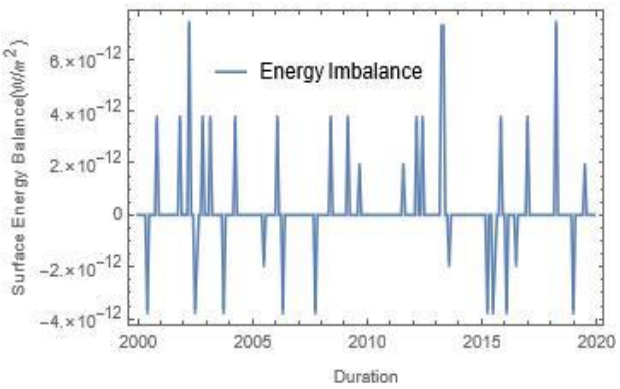

Figure 4. Time series of annual surface energy imbalance for Mubi during 2000-2020

4. Conclusion

It was concluded that the results based on the SEB components are in agreement with its stated equations, thereby revealing the amount of incoming and outgoing energy in the Mubi Earth surface in inferences to long-term trends. It was also found that the seasonal variation results obtained is highly influenced by local precipitation, evapotranspiration, soil and air temperature, which might be affected by incoming solar radiation, rainfall, or other related-meteorological conditions such as albedo, soil moisture, wind speed, soil temperature. The information provided in this study would help in planning, decision-making, and assessing the changes in SEB, which can comprehensively explore the recent seasonal changes and weather conditions over Mubi.

Acknowledgments

The authors are extremely grateful to the meteoblue AG, Basel, Switzerland, for providing us with the necessary data to carry out the present work.

Ethical issue

The authors are aware of and comply with best practices in publication ethics, specifically concerning authorship (avoidance of guest authorship), dual submission, manipulation of figures, competing interests, and compliance with policies on research ethics. The authors adhere to publication requirements that the submitted work is original and has not been published elsewhere in any language.

Data availability statement

Data sharing does not apply to this article as no datasets were generated or analyzed during the current study.

Conflict of interest

The authors declare no potential conflict of interest.

References

[1] M. Rahman, and W. Zhang, "Review on estimation methods of the Earth's surface energy balance components from ground and satellite measurements,'' J. Earth Syst. Sci. 128:84, 2019. https://doi.org/10.1007/s12040-019-1098-5.

[2] Y. Zhu, M, Ludwig, E. M., Cherkauer, "Estimation of Corn Latent Heat Flux from High Resolution Thermal Imagery," Remote Sens., 14, 2682. 2022. https://doi.org/10.3390/rs14112682.

[3] H. Hoffmann, H. Nieto, R. Jensen, R. Guzinski, P. Zarco-Tejada, T. and Friborg, "Estimating Evaporation with Thermal UAV Data and Two-Source Energy Balance Models," Hydrol. Earth Syst. Sci.; 20, 697–713, 2016.

[4] A. Imanian, M. H. Tangestani, A. Asadi, and M. Zare, "Calculation of Real Evapotranspiration by the Application of Metric Method on Landsat-8 Data," IOP Conf. Series: Earth and Environmental Science, 767 (2021) 012047. doi:10.1088/1755-1315/767/1/01204

[5] G. R. North, "Theory of energy-balance climate models," Journal of the Atmospheric Sciences, 32(11), 2033-2043, 1975.

[6] R. Tang, Z. Li, Y. Jia, C. Li, K-S. Chen, X. Sun and J. Lou, "Evaluating one- and two-source energy balance models in estimating surface evapotranspiration from Landsat-derived surface temperature and field measurements," International Journal of Remote Sensing, 2012. https://doi.org.10.1080/01431161.2012.716529

[7] K. Dintwe, G. S. Okin, and Y. Xue, "Fire-induced albedo changes and surface radiative forcing in sub-Saharan Africa savanna ecosystems: Implications for the energy balance," J. Geophys. Res. Atmos., 122, 6186–6201, 2017.

[8] R. A. Pielke, G. Marland, R. A. Betts, T. N. Chase, J. L. Eastman, J. O. Niles, D. D. S. Niyogi, and S. W. Running, "The influence of land-use change and landscape dynamics on the climate system: relevance to climate-change policy beyond the radiative effect of greenhouse gases," Philosophical Transactions A 360 (1797), 1705, 2002.

[9] M. O. Audu, B. C. Isikwue, and J. E. Eweh, "Estimation of Seasonal and Annual Albedo of the Earth's Atmosphere over Kano, Nigeria," IOSR Journal of Applied Physics (IOSR-JAP). 6(5): 56-62. 2014. www.iosrjournals.org

[10] X. Zhang, S. Liang, K. Wang, L. Li, and S. Gui, "Analysis of global land surface shortwave broadband albedo from multiple data sources. IEEE J. Special Topics Appl. Earth Observations Remote Sens. 2010.

[11] S. Liang, K. Wang, X. Zhang, and M. Wild, "Review on Estimation of Land Surface Radiation and Energy Budgets from Ground Measurement, Remote Sensing and Model Simulations," IEEE Journal if Selected Topics in Applied Earth Observations and Remote Sensing. 3(3): 225-240. 2010.

[12] W. G. M. Bastiaanssen, "SEBAL-based sensible and latent heat fluxes in the irrigated Gediz Basin, Turkey." J. Hydrol., 229, 87–100. 2000.

[13] M. Tasumi, "A review of evaporation research on Japanese lakes." Proc. ASCE/EWRI World Water and Environmental Resources Congress, ASCE, Reston, Va. 2005.

[14] R. G. Allen, M. Tasumi, and R. Trezza, "Satellite-Based Energy Balance for Mapping Evapotranspiration with Internalized Calibration (METRIC) – Model," Journal of Irrigation and Drainage Engineering. Pp. 380-394. 2007. https://doi.org/10.1061/Asce0733-94372007133:4380.

[15] W. G. M. Bastiaanssen, M. Menenti, R. A. Feddes, And A. A. M. Holtslag, "A remote sensing surface energy balance algorithm for land (SEBAL) 1. Formulation". Journal of Hydrology, 212–213, pp. 198–212, 1998.

[16] W. Brutsaert, "On a derivable formula for long-wave radiation from clear skies," Water Resources Research, 11:742–744. 1975.

[17] J. Schulz, G. Vogel, C. Becker, S. Kothe, U. Rummel, and B. Ahrens, "Evaluation of the ground heat flux simulated by a multi-layer land surface scheme using high-quality observations at grass land and bare soil," Meteorologische Zeitschrift, 25(5): 607–620, 2016.

[18] A. Usman, J. A. Sunday, and L. A. Sunmonu, "Estimation of the Ground Heat Flux from Percentage of Net Radiation in Ile-Ife, Osun State, Nigeria," International Journal of Research and Innovation in Applied Science (IJRIAS), VI(II): 101-105, 2021. www.rsisinternational.org

[19] W. P. Kustas, and C. S. T. Daughtry, "Estimation of the soil heat flux/net radiation ratio from spectral data,"

Agriculture and Forest Meteorology, 49, pp. 205–223. 1990.

[20] T, Chang, Y. Liou, C. Lin, S. Liu, and Y. Wang, "Evaluation of surface heat fluxes in Chiayi plain of Taiwan by remotely sensed data," International Journal of Remote Sensing. 31(14): 3885–3898, 2010.

[21] S. Bid, "Change Detection of Vegetation Cover by NDVI Technique on Catchment Area of the Panchet Hill Dam, India," International Journal of Research in Geography (IJRG), 2(3): 11-20, 2016. https://dx.doi.org/10.20431/2454-8685.0203002.

[22] V. Zuzulova, and J. Vido, J. "Normalized difference vegetation index (NDVI) as a tool for the evaluation of agricultural drought," Ecocycles, 4(1): 83-87, 2018. https://doi.org/ 10.19040/ecocycles.v4i1.124

[23] Y. Julien, J. A. Sobrino, C. Mattar, A. B. Ruescas, J. C. Nez-Munoz, G. S. Oria, V. Hidalgo, M. Atitar, B. Franch, and J. Cuenca, "Temporal analysis of normalized difference vegetation index (NDVI) and land surface temperature (LST) parameters to detect changes in the Iberian land cover between 1981 and 2001," International Journal of Remote Sensing, 32(7): 2057–2068, 2011. https://doi.org/10.1080/01431161003762363

[24] U. S. Geological Survey, "NDVI, the Foundation for Remote Sensing Phenology. 2015. Available at: http://phenology.cr.usgs.gov/ndvi_foundation.php

[25] A. C. Floyd, and A. E. Ruth, "Normalized Difference Vegetation Index (NDVI) Assessment of Vegetation Around Oben Gas Flow Station, Edo State, Nigeria," NIPES Journal of Science and Technology Research, 4(1): 311-321, 2022. Available at: https://nipesjournals.org.ng

[26] H. Khaleghi, H. Farani and M. Ahmadi, "A comparative study of breakup models in diesel fuel spray," The 25th Annual International Conference on Mechanical Engineering ISME 2017, 2-4 May 2017, Tarbiat Modares University, Tehran, Iran.

[27] A. Rostamijavanani, "Dynamic buckling of cylindrical composite panels under axial compressions and lateral external pressures," J Fail. Anal. and Preven. 21, 97–106, 2021. https://doi.org/10.1007/s11668-020-01032-3.

[28] S. Sultana, and A. N. V. Satyanarayana, "Impact of Urbanization on Surface Energy Balance Components over Metropolitan Cities of India during 2000–2018 winter seasons," Research Square, 2021. https://doi.org/10.21203/rs.3.rs-709565/v1

[29] Y. Ma, "Determination of regional surface heat fluxes over heterogeneous landscapes by integrating satellite remote sensing with boundary layer observations, PhD thesis, Wageningen University, Wageningen, The Netherlands, 2006.

[30] Y. Ilhamsyah, "Surface Energy Balance in Jakarta and Neighboring Regions as Simulated Using Fifth Mesoscale Model (MM5)," Aceh Int. J. Sci. Technol., 3(1): 27-36, 2014. https://doi.org/10.13170/AIJST.0301.03

[31] X. Liu, "Surface Energy and Mass Balance Model for Greenland Ice Sheet and Future Projections," A dissertation submitted in partial fulfillment of the requirements for the degree of Doctor of Philosophy (Atmospheric, Oceanic and Space Sciences) in The University of Michigan, 2017.

[32] H. Wang, and J. Ma, "Analysis of Land Surface Energy and Water Cycle Changes in Naqu Region of Qinghai-Tibet Plateau during 2005-2016," Open Access Library Journal, 8: e7670, 2021. https://doi.org/10.4236/oalib.1107670

[33] Y. Petchprayoon, "Analysis of Climate Change Impacts on the Surface Energy Balance of Lake Huron. (Estimation of Surface Energy Balance Components: Remote Sensing Approach for Water - Atmosphere Parameterizations," A thesis submitted to the Department of Geography, Faculty of the Graduate School of the University of Colorado in partial fulfilment of the requirement for the degree of Doctor of Philosophy. 2015.

[34] O. Akuoko, "Surface energy balance partitioning in tilled and non-tilled bare soils," A thesis submitted to the graduate faculty in partial fulfillment of the requirements for the degree of Master of Science, Department of Environmental Science, Iowa State University Ames, Iowa, 2018.

[35] U. Kumar, C, Rashmi, and S. N. Raghuwanshi, "Comparative Evaluation of Simplified Surface Energy Balance Index-Based Actual ET against Lysimeter Data in a Tropical River Basin. Sustainability, 13, 13786, 2021. https://doi.org/10.3390/su132413786

[36] E. E. Small, and S. Kurc, "Simulating summertime rainfall variability in the North American monsoon region: The influence of convection and radiationparameterizations," Journal of Geophysical Research, Vol. 107, NO. D23, 4727, doi:10.1029/2001JD002047. 2001.

[37] R. Hock, and B. Holmgren, "A distributed surface energy-balance model for complex topography and its application to Storglacia¨ren, Sweden. Journal of Glaciology, 51(172): 25-36, 2005.

[38] E. Bäckström, "The surface energy balance and climate in an urban park and its surroundings," Department of Earth Sciences, Uppsala University Villavägen 16, 752 36 Uppsala, Sweden, 2006. ISSN 1401-5765.

[39] A. Verhoef, J. S. Allen, and R. Lloydc, "Seasonal variation of surface energy balance over two Sahelian surfaces," International Journal of Climatology. 19: 1267–1277, 1999.

[40] S. P. Arya, "Introduction to Micrometeorology," (2nd ed). California USA: Academic Press, 2001. Hardcover ISBN: 9780120593545.

[41] E. Nwaokoro, and E. F. Nymphas, "TEMPERATURE VARIATIONS AND SOIL THERMAL PROPERTIES AT THE NIGERIA MESOSCALE EXPERIMENT SITE, IBADAN, NIGERIA," International Research Journal of Pure and Applied Physics. 7(1): 7-14, 2020.

[42] A. T. Akinseloyin, "Soil Moisture and Temperature Simulation Using the Versatile Soil Moisture Budget Approach," A Thesis submitted to the Faculty of Graduate studies of the University of Manitoba in partial fulfilment of the requirements for the degree of Master of Science, Department of Soil Science, University of Manitoba, 2015.

[43] P. Pramanik, K. K. Bandyopadhyay, D. Bhaduri, B. Bhaacharyya, and P. Aggarwal, "Effect of mulch on soil thermal regimes - A review. International Journal of Agriculture, Environment and Biotechnology (IJAEB), 8(3): 645-658, 2015. https://doi.org./10.5958/2230-732X.2015.00072.8.

[44] T. Adak, S. Gopalkumar, P. K. Srivastava, and N. V. K. Chakvawarty, "Seasonal changes in Soil Temperature within Mustard Crop Stand," Journal of Agro Meteorology. 13: 72-74, 2011.

[45] T. Adak, and N. V. K. Chakravarty, "Relation between Soil Temperature and Biophysical Parameters in Indian Mustard Seeds," International Journal of Agronomic Physics. 27: 359-367, 2012.

[46] C. M. Jacobs, A. F. Jacobs, F. C. Bosveld, D. M. Hendriks, and E. M. Veenendaal, "Variability of Annual CO2 Exchange from Dutch Grasslands," Journal of Bio. Geo Physical Science. 4: 803-16, 2007.

[47] L. Jens, and J. Fuhrer, "The Temperature Response of CO2 Production from Bulk Soils and Soil Fractions is related to Soil Organic Matter Quality," Journal of Bio. Geo Chemistry. 75 (3): 433-453, 2005.

[48] A. A. Alli, and O. E. Omofunmi, "A Review of Soil Temperature Under a Controlled Irrigation System," Journal of Research in Forestry, Wildlife & Environment, 13(1): 50-59, 2021.

[49] A. Melkonyan, "Climate change impact on water resources and crop production in Armenia," Agricultural Water Management, 161, 86-101, 2015.

[50] V. Potopova P. Zahradnicek P. Stepanek L. Turkott A Farda and J. Soukup "The impacts of key adverse weather events on the field-grown vegetable yield variability in the Czech Republic from 1961 to 2014," International journal of Climatology, 37:1648-1664, 2017.

[51] A. Mansur, "The Impact of Soil Temperature on Miscanthus (Elephant) Plant: A Case study of Compton Experimental Site, West Midlands, UK. International Journal of Science and Research (IJSR), 4(4): 2104-2108, 2015. Available at: www.ijsr.net.

[52] M. O. Kehinde, and A. T. Umar, "Assessment of Soil Moisture Storage In Nigeria Using Climatic Water Budgeting Approach," Ghana Journal of Geography, 13(1): 167-202, 2021. https://dx.doi.org/10.4314/gjg.v13i1.9

[53] Y. Liou, and S. K. Kar, "Evapotranspiration Estimation with Remote Sensing and Various Surface Energy Balance Algorithms—A Review," Energies 2014, 7, 2821-2849; https://doi.org/10.3390/en7052821.

[54] A. Pereira, and L. Pires, "Evapotranspiration and Water Management for Crop Production," InTech. Pp. 143-166, 2011. https://doi.org/10.5772/20081

[55] P. Wang, X. Song, D. Han, Y. Zhang, and B. Zhang, "Determination of evaporation, transpiration and deep percolation of summer corn and winter wheat after irrigation. Agric. Water Manag., 105, 32–37, 2012.

[56] P. Bogawski, and E. Bednorz, "Comparison and Validation of Selected Evapotranspiration Models for Conditions in Poland (Central Europe). Water Resour. Manag., 28, 5021–5038, 2014.

[57] S. Wanniarachchi, and R. A. Sarukkalige, "Review on Evapotranspiration Estimation in Agricultural Water Management: Past, Present, and Future," Hydrology, 9, 123, 2022. https://doi.org/10.3390/hydrology9070123

[58] J. B. Winbourne, T. S. Jones, S. M. Garvey, J. L. Harrison, L. Wang, D. Li, P. H. Templer, and L. R. Hutyra, "Tree Transpiration and Urban Temperatures: Current Understanding, Implications, and Future Research Directions," BioScience, 70, 576–588, 2020.

[59] S. A. Salman, S. Shahid, H. A. Afan, S. M. Shiru, N. Al-Ansari, and Z. M. Yaseen, "Changes in Climatic Water Availability and Crop Water Demand for Iraq Region," Sustainability, 12, 3437, 2020.